International Conference on Space Optics—ICSO 2004

Toulouse, France

30 March–2 April 2004
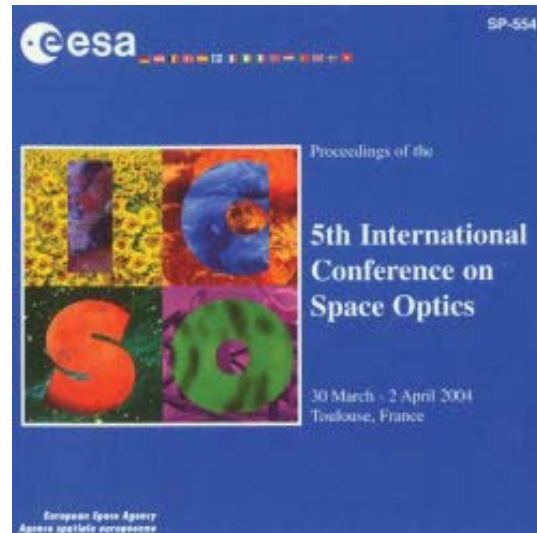
The IASI detection chain

Patrick Nicol, Joel Fleury, Claire Le Naour, Frédéric Bernard

THE IASI DETECTION CHAIN

Patrick NICOL [(1)], **Joel FLEURY** [(2)], **Claire LE NAOUR** [(3)], **Frédéric BERNARD** [(3)]

(1) ALCATEL SPACE – 100 bd. du midi 06156 Cannes la Bocca France- email *: patrick.nicol@space.alcatel.fr*
(2) SAGEM SA – Le Ponant de Paris – 27, rue Leblanc 75512 PARIS Cedex15 email : joel.fleury@sagem.com
(3) CNES – 18 av. Edouard Belin 31401 Toulouse France- email : frederic.bernard@cnes.fr

ABSTRACT

IASI (Infrared Atmospheric Sounding Interferometer) is an infrared atmospheric sounder. It will provide meteorologist and scientific community with atmospheric spectra. The instrument is composed of a Fourier transform spectrometer and an associated infrared imager.

The presentation will describe the spectrometer detection chain architecture, composed by three different detectors cooled in a passive cryo-cooler (so called CBS : Cold Box Subsystem) and associated analog electronics up to digital conversion. It will mainly focus on design choices with regards to environment constraints, implemented technologies, and associated performances .

CNES is leading the IASI program in collaboration with EUMETSAT. The instrument Prime is ALCATEL SPACE responsible, notably, of the detection chain architecture. SAGEM SA provides the detector package (so called CAU : Cold Acquisition Unit).

1- INTRODUCTION

Since years, Earth Observation needs even higher performance detection systems. For IASI application, the use of passive cryo-cooler leading to an operational temperature range of the focal plane up to 100 K makes it even more challenging, as all the performance has to be achieved until 15.5 µm.

This challenge is now successfully reached thanks to intensive development made at detector level and also to the very efficient passive cryocooler developed by ALCATEL SPACE [1] with an achieved on-ground temperature of 93 K.

Fig. 1. Detectors integrated in Cold Box

2- DETECTION CHAIN MAIN REQUIREMENTS

The IASI spectral domain is from 645 to 2760 cm^{-1} (3.62 to 15.5 μm). The Radiometric noise performance is specified in terms of Noise Equivalent Temperature Difference (NETD), with a scene equivalent to a blackbody temperature of 280 K. Requirement synthesis is presented in table 1.

Wave Number domain [cm^{-1}]	Noise
$645 \leq \sigma < 650$	0.33 K
$650 \leq \sigma < 770$	0.28 K
$770 \leq \sigma < 1000$	0.33 K
$1000 \leq \sigma < 1070$	0.28 K
$1070 \leq \sigma < 1210$	0.33 K
$1210 \leq \sigma < 1650$	0.28 K
$1650 \leq \sigma < 2100$	0.58 K
$2100 \leq \sigma < 2150$	0.47 K
$2150 \leq \sigma < 2250$	0.47 K
$2250 \leq \sigma < 2350$	0.58 K
$2350 \leq \sigma < 2400$	0.47 K
$2400 \leq \sigma < 2420$	17 μW/m² sr cm^{-1}
$2420 \leq \sigma < 2760$	20 μW/m² sr cm^{-1}

Table 1 : IASI NETD requirements

IASI field of view is sampled by 4 pixels for which homogeneous performance is necessary. At last, uniformity and signal phasing (the useful signal is between 17 and 80 kHz) were also performances necessary to manage.

3 - DETECTION CHAIN ARCHITECTURE

The detection chain is composed of the Cold Acquisition unit (CAU) - 3 detector packages (B1/B2/B3) covering IASI spectral band - and the Main Acquisition Subsystem (MAS) – providing detectors polarisation, gain / offset correction and numerization.
At this stage, detector bias, preamplifier and amplifier gains, and offset correction have been defined and are adjusted during instrument integration in order to optimise signal to noise ratio.

A schematic view of the detection chain is given in fig. 2. CAU description and performances are presented in details in chapter 4. A synthesis of MAS and Signal phasing description is presented in the following subsections.

Detectors' preamplifier place has been optimised regarding noise and impedance constraints:
- in B1, the PA needs to be very noiseless, and this performance ($\approx$1nV/$\sqrt{\text{Hz}}$) could only be achieved

with bipolar transistors which need a minimum ambient temperature to work properly. So, we chose to put it in the MAS,
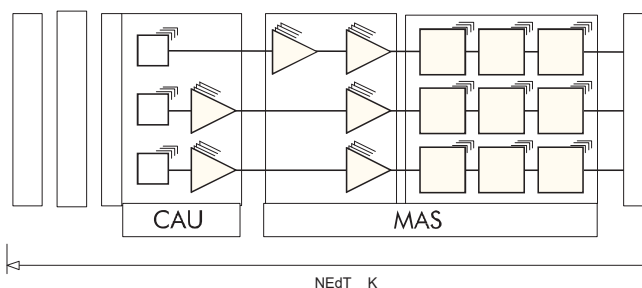

NEdT K
Fig. 2. : Detection chain architecture

- in B2/B3, the very high detector impedance needs the proximity of a PA. So, the cryogenic temperature implies to use CMOS technology. CNES developed for this application an ASIC with very low noise level ($\approx$10nV/$\sqrt{\text{Hz}}$), because at development time not cots with required performance was available .

While performance optimisation in B2/B3 is limited to a gain/offset adaptation during instrument integration (achieved at lower level), in B1 a trade-off has to be performed for polarisation selection taking into account detector D*, CBS temperature sensitivity to CAU dissipation and MAS noise. This trade-off is done based on equipment characterisation and also through the test campaign performed at CBS level.

3.1   MAS description

The MAS sub-system has for principal function to digitalize the signals incoming from detectors. The general structure of the MAS is based on a architecture by pixel. The pixel is composed of three acquisition chains (B1/B2/B3), a DC/DC converter and interface circuit common to the chains. Every chain receives an analog signal from CAU. This signal is pre-amplified, amplified, filtered and converted in digital data.
The signals from detectors B1 and B2/B3 have different electrical characteristics. The preamplifier normalises these signals in order to have the same dynamic range for the twelve detection chains at next stage.

For each pixel the functions of the preamplifier are :
- to filter the incoming signals from CAU (through the cold links) towards EM perturbations,
- to provide bias voltage to the B1 detector (5 bias voltage available) and compensate the bias current of B1 detector,
- to compensate the B1 offset and notably their drifts thanks to tele-command,

- to make current/voltage conversion and to amplify with very low noise the B1 useful signal.

This function encloses a device which reduces the static linearity error resulting from the serial resistance of the cold link between the detector and the MAS.

- to amplify the differential signals incoming from B2/B3 detector with low noise.

- to transmit B1/B2/B3 signals to the ADC with low impedance.

- to deliver power supply to the B2/B3 hybrid preamplifiers.

The next stage aims to amplify, to subtract offset (for B2 and B3 band) and to filter the analog signal from the preamplifier. The latter consists in an anti aliasing filter which aims to reduce the noise. All those functions are also provided by an analog ASIC.

The last stage aims to convert the twelve analog signals incoming from the analog signal processing. The ADC is an AD1671 allowing 12 bits quantization. To improve performance and thanks to the very special shape of the interferogram signal (fig. 3), the ADC includes 2 automatic switchable gains (gain 4 and 16) which allow to get an equivalent 16 bits quantization . All the functions of the automatic gain adjustment of the ADC are performed by an ASIC.
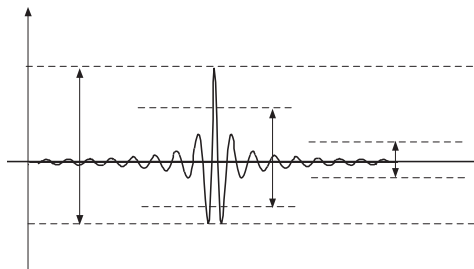

Fig. 3 : Sampling resolution

These numerical data are formatted and multiplexed to be transmitted with a high speed data link (LNR) to the Digital Processing Subsystem (DPS).

The MAS consists in one single box containing 10 boards stacked vertically and a mother board.

The size of the box is 300x300x230 mm^3 for a mass of 11 kg

3.2   RPD phasing with useful signal

The Reference Path Difference (RPD) signal is a precise reference indicating the value of the Optical Path Difference (OPD) during the interferometer cube corner motion. Its frequency is around 346 kHz. It is used as a sampling reference Clock for the analog to digital conversion during the acquisition of the

interferograms. As OPD is not stable during cube corner motion, both signals (useful signal and RPD) have to be perfectly synchronised in order to avoid error.

Fig. 4 presents the different contributors which introduce delays on both signals
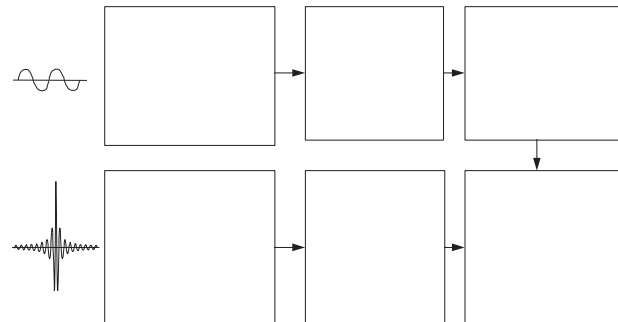

Fig. 4 : RPD phasing with useful signal

The delay on the analog useful signal, before reaching the ADC stage, is due to hybrid preamplifier in the CAU, amplifier in the MAS, and mainly to the anti-aliasing filter (AAF) in the MAS. It introduces an important delay (around 3.5 µsec) compared to RPD channel, which require to introduce a constant delay in the RAU to roughly compensate this difference.

A fine adjustment is done through a tuneable delay available in the MAS, which allows to compensate for manufacturing and knowledge errors on the different contributors. It has been successfully validated during IASI instrument PFM test.

4 - CAU DESCRIPTION

The CAU consists in 3 independent detector packages, one for each spectral band (B1, B2 and B3) of the IASI instrument.

PV focal plane (B2 & B3) arrays are provided with hybrid preamplifiers because the output signals are low-level and the output impedances are very high. The definition of the useful spectral band is given below :

	$\lambda_{min}(\mu m)$	$\lambda_{max}(\mu m)$	Detector Mode	Material
B1	8.26	15.5	Photoconductive	HgCdTe
B2	5	8.26	Photovoltaic	HgCdTe
B3	3.4	5	Photovoltaic	InSb

Each detector package consists in 2x2 elements array mounted on a detector substrate behind four microlenses. The pixel size of one detector is 0.9 mm square and distance between detectors centres is 2.24 mm. The microlenses conjugate aperture stop with detectors to concentrate flux and to improve system spatial non uniformity. Positioning accuracy of the detectors and microlenses is measured at ambient temperature with an accuracy better than 5 µm.

Each B2 and B3 detector package contains an hybrid circuit with four ASIC CMOS cryogenic amplifiers, developed by CNES (in the Opto-Electronic Department). The hybrid circuit allows to amplify the signals as near as possible from the detectors. Signals are then transmitted to the MAS which is at a temperature of about 293 K through a 600 mm flexible cold link.

4.1. Configuration of the detector packages

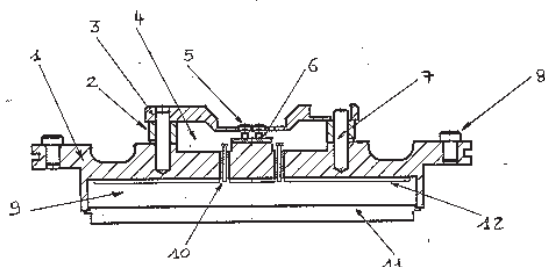The configuration of the B2/B3 detector packages is given in the figures below :

Figure 5 : B2/B3 detector package assembly
1. *Baseplate in Dilver*
2. *Adjustable frame for the distance "detectors-microlenses"*
3. *Microlenses support*
4. *Non hermetic optical cavity*
5. *Microlenses*
6. *Detectors*
7. *Microlenses automatic self centering on the baseplate*
8. *Baseplate automatic self centering on the CBS*
9. *Hermetic hybrid cavity*
10. *Feed-throughs by DIL connections*
11. *Hybrid cover*
12. *Hybrid substrate*
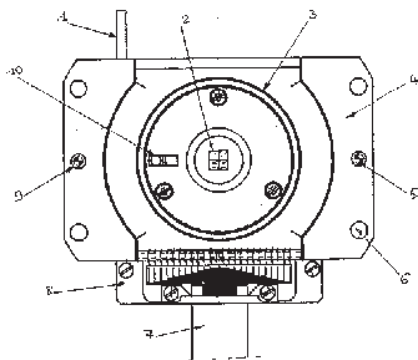
Figure 6 : B2/B3 detector package front face
1. *Suck off tube*
2. *Microlenses*
3. *Microlenses support*
4. *Baseplate*
5. *Baseplate automatic self centering on the CBS*
6. *Fixation holes*
7. *Cold link*
8. *Cold link electrical and mechanical interface*
9. *Baseplate automatic self centering on the CBS*

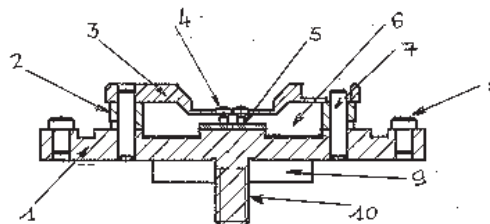The configuration of the B1 detector package is given in the figures below :

Figure 7 : B1 detector package assembly
1. *Baseplate in Dilver*
2. *Adjustable frame for the distance "detectors-microlenses"*
3. *Microlenses support*
4. *Microlenses*
5. *Detectors*
6. *Non hermetic optical cavity*
7. *Microlenses automatic self centering on the baseplate*
8. *Baseplate automatic self centering on the CBS*
9. *Feed-throughs by DIL connections*
10. *Thintening nut for thermical strap*

4.2. Detector design

For each band, the IR detection is made by a monolithic 2 x 2 detector array with a cutting up in the middle to separate the detectors. So, the four detectors are electrically isolated and the relative positioning of the detectors is perfect in the X,Y,Z axes.

B1 photoconductive detectors are processed by SAGEM on high performance epitaxial MCT thick film material manufactured by SOFRADIR.
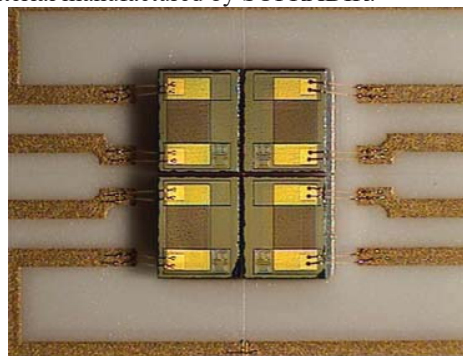
Figure 8 : B1 detector array

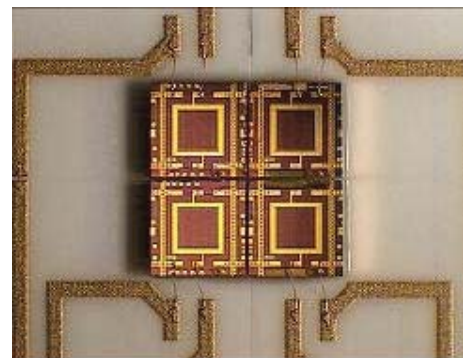B2 photovoltaic detectors are processed by SAGEM on its own MCT wafers.

Figure 9 : B2 detector array

B3 photovoltaic detectors are processed by SAGEM on InSb wafers manufactured by JOHNSON MATTHEY.
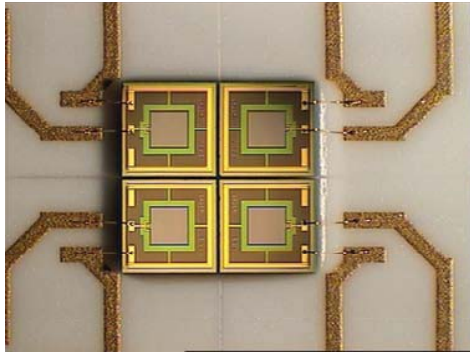
Figure 10 : B3 detector array

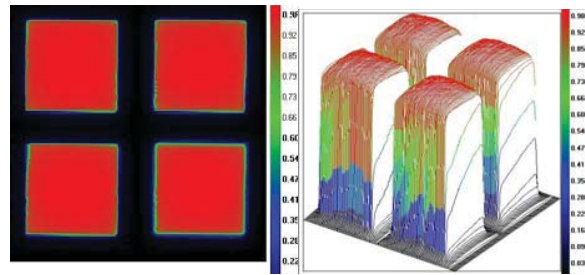|	Fmin	Fmax
B1	17 kHz	37 kHz
B2	29 kHz	60 kHz
B3	50 kHz	79 kHz

Figure 13 : B3 detector array spot scan (80 K)

The main difficulty for the B1 detector process is due to the high level of detectivity specified in the 8.5 to 15.5 µm spectral band, at 100 K. An other difficulty is due to the spatial uniformity which is not so good with PC technology comparing with PV technology and which requires a screening of the detectors. For B2 detectors, the main difficulty is due to the dark current at 100K which must not saturate the preamplifier and which requires a screening of the cut-off wavelength.

4.3. Detector performances

The following figures (11 to 13) show the spatial uniformity achieved performance with good homogeneity on the 2x2 array.

Figure 11 : B1 detector array spot scan (80 K)

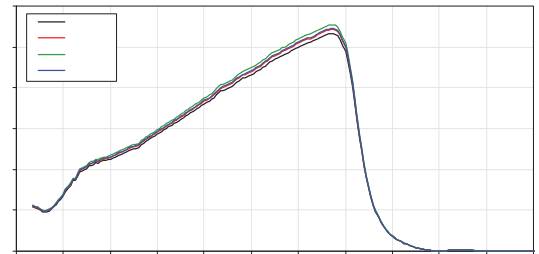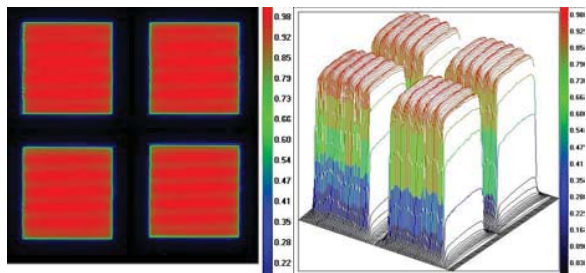**Figure 12 : B2 detector array spot scan (80 K)**

The detectivity in the figures 14 to 16 are given in Jones (cm.$\sqrt{Hz}$.W^{-1}) Signal is measured, at 100 K, in front of the radiation of a blackbody at 600°C, modulated at 1500 Hz. Noise is measured, at 100 K, in front of the radiation of a blackbody at 20°C in the dedicated electrical bands :

Figure 14 : B1 detector array spectral detectivity

Figure 15 : B2 detector array spectral detectivity
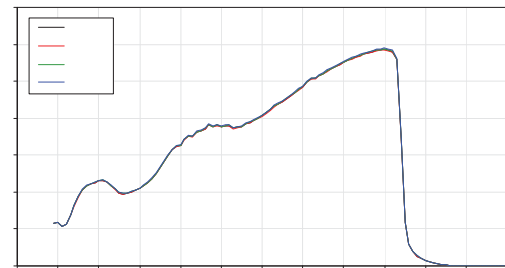
Figure 16 : B3 detector array spectral detectivity

Fig. 17, illustrates the criticality of B2 dark current evolution with temperature .
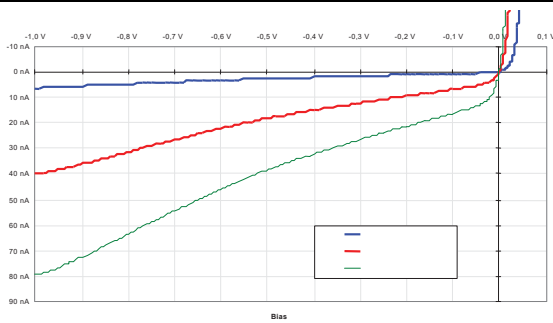
Figure 17 : I(V) curve of a typical B2 detector (90K-100 K-105K / dark ground)

4.4.   Microlens design

Microlenses are individually manufactured by mechanical machining with diamond point, in Germanium material.
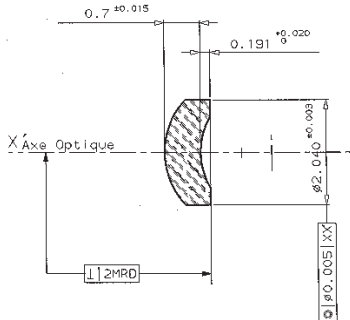

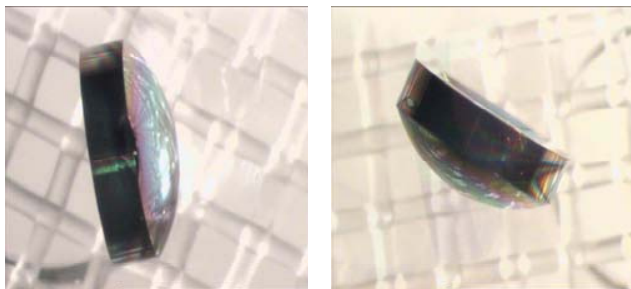**Figure 18 : IASI microlens definition**

Figure 19 : microlens photographs

4.5.   Microlens performances

Image quality : the maximum irregular component of the wavefronts reflected by the optical surfaces is better than 2 µm PTV on the full pupil.

Roughness : the maximum RMS roughness of the optical surfaces is lower than 10 nm.

Spectral transmissions : they have been measured, for B1, B2 and B3, on plane witnesses, on normal incidence, at 300 K and 100K. Influence of the incident rays until a angle of incidence of 40° has also been measured.

Fig. 20 shows B1 microlens spectral transmission with main difficulty at 15 µm due to germanium absorption .

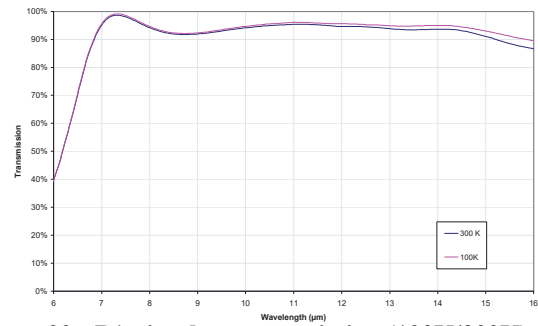For B2 and B3 bands achieved transmission in the whole useful spectral band is higher than 0.95 .

Figure 20 : B1microlens transmission (100K/300K)

4.6.   Microlenses assembly

The microlenses are mounted by gluing in the aperture of a titanium support as shown in fig. 21 & 22.

This aperture is realised with a very high precision. The edges of the aperture constitute the reference axes for the microlenses. Positioning control of the microlenses support on the baseplate is made by visual projection with a magnitude of 100.

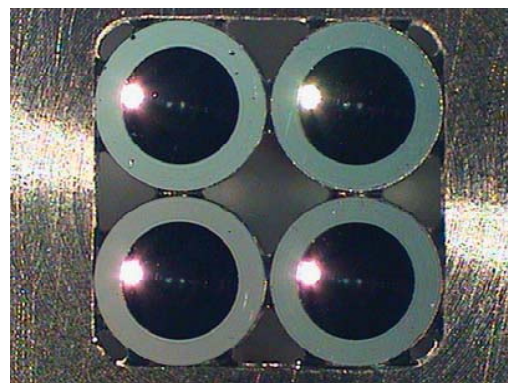**Figure 21 : microlenses support (front face)**

Figure 22 : microlenses support (back face)

4.7.   Hybrid cavity design

The preamplifiers are realised with low temperature hybrid technology. Four PA substrates, equipped with an ASIC and peripheral thick film resistors are mounted on a main substrate equipped with the capacitors. All the substrates and components are hold

by isolating or conductive glues. The electrical connections are made by gold wire ultrasonic ball bonding. The low noise ASIC was developed by CNES and manufactured by ES2 company in a 0.7µm CMOS process. Screen printed substrates and thick film resistors have been manufactured by SAGEM.

The hybrid cavity is hermetic. The cover is reported by laser wedge and the cavity is pumped via a suck off tube. An helium pressure of 0.5 bar is introduced in the cavity before closing the suck off tube.
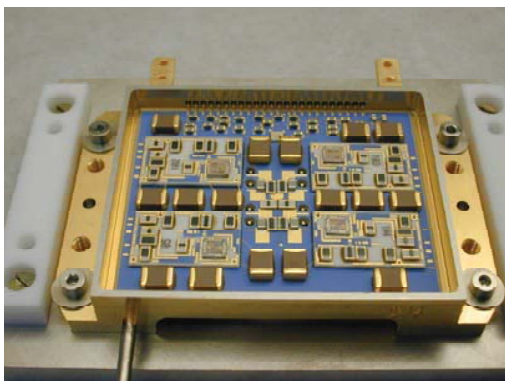

Figure 23 : hybrid cavity photograph

4.8. B2/B3 electrical circuits

The B2/B3 trans-impedance circuits take into account the adjusment between detector and preamplifier as well as the EMC constraints with the detector and the cold link (see fig. 24). On the main substrate, a 2N2222 transistor is used to control and to drive the detector package temperature.
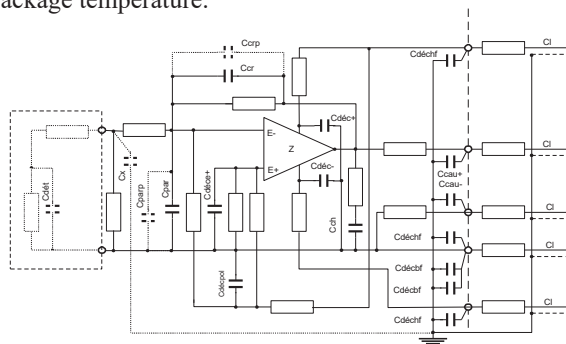

Figure 24 : B2/B3 electrical scheme

4.9. Cold links

The cold links have been studied specially for the IASI application in terms of electrical resistance and capacitance, electromagnetic compatibility, thermal transfer, flexible and rigid surfaces…

The cold links are interfaced with the detector packages by bonding and with the MAS by connectors. They are coupled to the three stages of the radiator of the cold box by thermalisation areas which are also fixation points. The shield is connected with the mechanical ground.
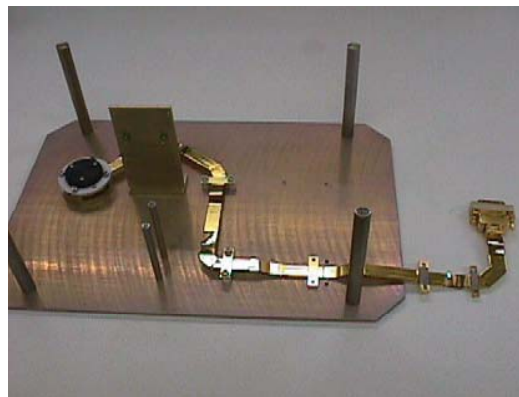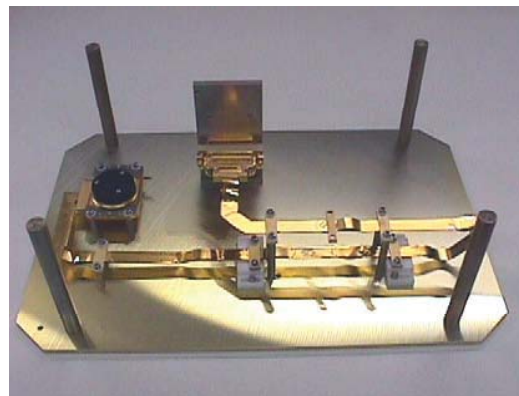

Figure 25 : B1 cold link view
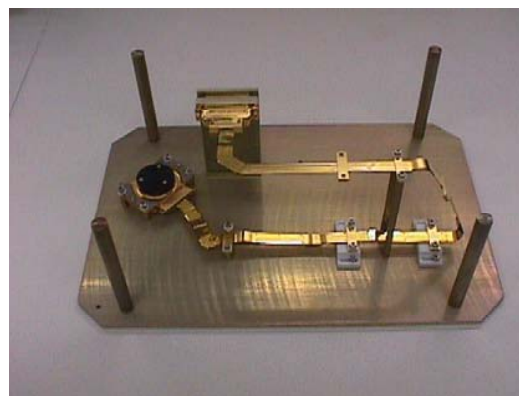

Figure 26 : B2 cold link view

Figure 27 : B3 cold link view

4.10. Integration of the detector packages

The different parts of the detector packages are mounted by screwing : the microlenses support, the adjustable intermediate frame and the cold link. The integration is very similar between B1 and B2/B3 packages.

The optical cavity is non hermetic The thermal coupling between the cold box and the detector packages is induced by contact at the mechanical interface. The reference for the positioning of the detector packages on the cold box are given by two self-centring pins.
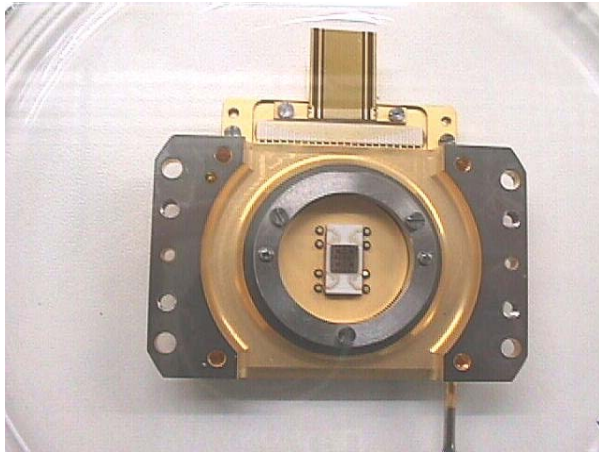
Figure 28 : view of the B2/B3 optical cavity

Figure 29 : B2/B3 equipped detector package

5 – DEVELOPMENT STATUS

The detection chain validation has been performed in four steps. A first performance verification, early in the development, with breadboard models of CAU and MAS, has allowed to check MAS functionality , signal and noise evolution with temperature and scene.

Then, sensibility to EMC environment (E-Field and H-Field) has been characterised with CAU integrated in a dummy CBS (see fig. 30). Main concern was related to grounding loop linked to cold link routing in CBS.
These tests have allowed to identify critical environment, to introduce modification in CAU design and to prepare grounding trade-off at CBS level.

The two following steps have been performed during instrument PFM integration through optical vacuum tests at CBS and instrument level.
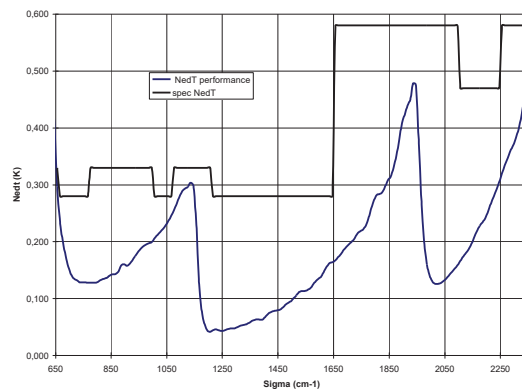
Signal and noise achieved performances have been

measured in accordance with radiometric prediction models what allow to validate it.

Figure 30 : Detection chain EMC test

FM2 instrument is under integration with, notably, improved B1 detectors. Detection chain tests foreseen at very short term will allow to assess the fulfilment of

IASI mission requirements.

Figure 31 : IASI FM expected performance

6 – CONCLUSION

As shown in this paper , the IASI detection chain is made of numerous technologies which have all brought their development difficulties. Tight co-operation between CNES, SAGEM and ALCATEL SPACE experts has allowed to face them and to succeed in the achievement of IASI challenging performance at 15.5 µm.

7 – REFERENCE
 [1] B. Bailly, P. Courteau & T. Maciaszek, *The IASI cold box subsystem (CBS) A passive cryocooler for cryogenic detectors and optics*, ICSO 2000